ORIGINAL PAPER

CrossMark

Exchange Coupling in MnAlC/α-Fe Nanocomposite Magnets

J. S. Trujillo Hernandez[1,2] · F. Maccari[3] · L. G. Marshall[4] · Jesús A. Tabares[1] · G. A. Pérez Alcázar[1]

Abstract

Nanostructured composite materials consisting of exchange-coupled hard and soft magnetic phases are proposed as alternative for the development of high-energy product permanent magnets. In this work, we have examined the effects of soft magnetic α-Fe addition on the structure and magnetic properties of powders composed of hard magnetic $Mn_{54.3}Al_{44}C_{1.7}$ compound. The optimum melt-spun ribbon precursor (with τ-phase structure, with magnetization of 88 emu/g and coercive field of 1.6 kOe) was obtained after annealing the ribbons at 500 °C for 20 min. After the combination between the soft and the optimized hard phase, the intensity of τ-phase peaks measured by X-ray diffraction decreases. These changes can also be seen in the magnetic properties. The coercivity ($\sim$ 500 Oe) tends to decrease with the annealing temperature, while the magnetization tends to increase up to 141 emu/g. Evidence of good exchange coupling between particles of $Mn_{54.3}Al_{44}C_{1.7}$ and α-Fe, in the produced composite, was proved by the hysteresis loop and its corresponding Thamm-Hesse analysis.

Keywords MnAlC alloys · Mössbauer spectroscopy · Cryomilling

1 Introduction

Recently, significant attention has been paid to the development of alternatives to supply permanent magnets, which are not based on rare earth (RE) elements, the so-called RE-free magnets. The high cost of RE elements makes the commercial application of this high-performance magnet very expensive. With the increasing demand of technology based on permanent magnets and the limited global supply of rare earths, the necessity for RE-free magnets has received wide-spread attention. In the available possibilities, Mn-based permanent magnets have been considered a promising system to fulfill some applications where the RE-based magnets are used [1]. In this context, the ferromagnetic τ-phase of the Mn–Al alloy [1, 2] has recently received a lot of attention due to the theoretical (BH)max value of $\sim$ 12 MGOe, high magnetization, relatively high magneto-crystalline anisotropy ($K_1 = 1.7$ MJ/m^3), low cost, low density (5 g/cm^3), and the possibility to large-scale production of bulk magnets [3, 4]. The τ-phase of Mn–Al (L10-type structure) is metastable and forms from the high-temperature ε-phase, which is stable above 800 °C. The addition of carbon to the τ-phase of the Mn–Al alloy has been proven to help stabilize the structure [4]. Besides the necessity of permanent magnet (PM) production without RE elements, there is also the need to improve the extrinsic magnetic properties. For this purpose, one strategy is to create exchange-spring or nanocomposite magnets [5, 6]. In such systems, a considerable amount of hard magnetic phase (MnAlC) is replaced by a soft magnetic phase (FeCo or α-Fe) and both phases are mixed at nanoscale to perform the concept of interphase exchange coupling [7]. Within this concept, the RE-free nanocomposite magnets can be tuned in terms of magnetic properties and also provide opportunities to reduce the cost of PMs considerably. In this work, we reported a process route towards the production of an exchange-spring magnet, combining RE-free alloy and a soft material, optimizing the microstructure and the magnetic properties.

✉ J. S. Trujillo Hernandez
  juan.sebastian.trujillo@correounivalle.edu.co

1 Departamento de Física, Universidad del Valle, Mélendez, Cali, A.A. 25360, Colombia

2 Facultad de Ciencias Naturales y Matemáticas, Universidad de Ibagué, Ibagué, Tolima, Colombia

3 Institute of Materials Science, Technische Universitaet Darmstadt, Alarich-Weiss-Strasse 16, 64287, Darmstadt Germany

4 Department of Chemical Engineering, Northeastern University, Boston, MA 02115, USA

Springer

2 Experiment

A $Mn_{54.3}Al_{44}C_{1.7}$ alloy ingot was prepared by arc melting using Mn, Al, and C of high purity (more than 99.9%) under an argon atmosphere, and the charges were melted two times to ensure homogeneity. Three weigh percent of Mn in excess was added to compensate the evaporation during the melting process. The resulting alloy ingot was then melt-spun using 750 mTorr Ar atmosphere, with a tangential velocity of the copper wheel of 30 m/s. After ribbon production, they were cryomilled using a SPEX 6770 Freezer/Mill in a LN2 bath (SPEX SamplePrep). Polycarbonate vials with stainless steel end-caps and a magnetically driven stainless steel impactor were used in this system. Samples were sealed in the vials under Ar atmosphere with 0.25 wt.% oleic acid added as surfactant [8]. Processing cycles consisted of 10 min of cryomilling at a rate of 15 cycles/s followed by 2 min of cooling. After cumulative milling time of 7 h, the surfactant was removed from the recovered powders by rising repeatedly with ethanol. The as-milled powder of $Mn_{54.3}Al_{44}C_{1.7}$ was encapsulated under a vacuum, in a quartz tube, followed

Fig. 1 XRD patterns of **a** $Mn_{54.3}Al_{44}C_{1.7}$ melt-spun ribbons, **b** $Mn_{54.3}Al_{44}C_{1.7}$ after annealing for 20 min at 500 °C and **c, d** $Mn_{54.3}Al_{44}C_{1.7}/\alpha$-Fe after cryomilling for 4 h and after annealing for 20 min at 500 and 600 °C. All brag peak are accounted for by τ-MnAl, ε-MnAl, and α-Fe phases
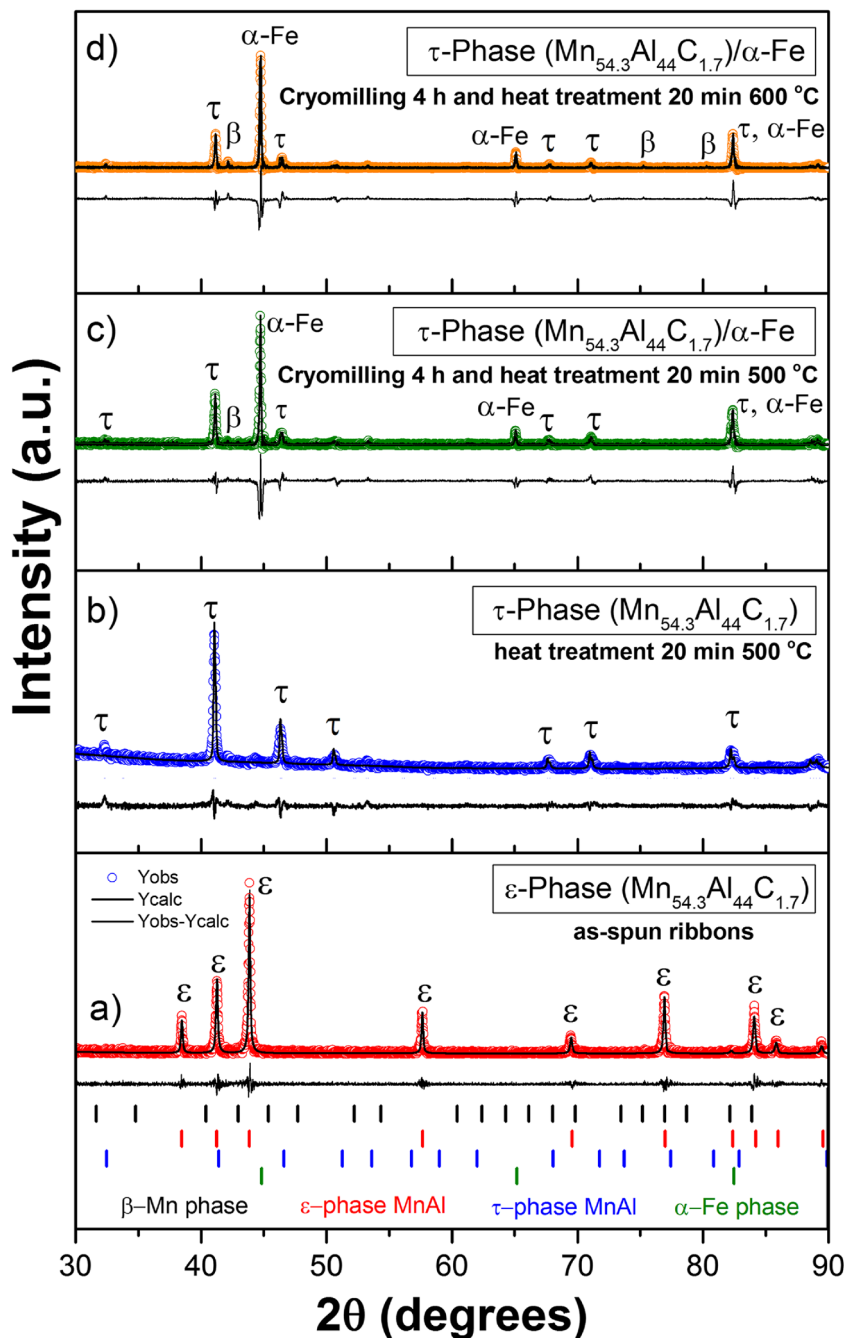
by annealing at 500 °C for 20 min followed by water quenching. Commercial high-purity α-Fe powder (more than 99.9% and mean particle size of ~ 100 μm) was submitted to similar cryomilling and then, the as-milled powders of $Mn_{54.3}Al_{44}C_{1.7}$ and α-Fe (20 wt.%) were mixed and cryomilled for an additional 4 h, then annealed at 500 and 600 °C in order to optimize the magnetic properties. The X-ray diffraction measurements were performed at room temperature using a PANalytical X'pert Pro diffractometer equipped with a Cu-Kα radiation. The patterns were refined by the Rietveld method combined with Fourier analysis using the GSAS software [9]. This procedure yielded the average values of the lattice parameter, crystallite size, and the structural phase ratios. The magnetic properties were measured using a LakeShore Vibrating Sample Magnetometer (VSM), at room temperature, under external magnetic fields up to 3 T. Demagnetization correction was made for the magnetic measurements. The Thamm-Hesse method was used to study the type of predominant interactions between particles. In order to evaluate the magnetic interaction, we use a simple relation, which is called the δM-plot, $\delta M = M_{init} - (1/2) \times (M_{up} + M_{down})$, where the M_{init}, M_{up}, and M_{down} are the magnetization values over the initial magnetization curve, upper, and lower part of the hysteresis loop, respectively, as described in [10]. Scanning electron microscopy (SEM) was used to follow the morphology of the samples during processing. The phase evolution of the samples were investigated by differential scanning calorimetry (DSC; Netzsch STA 449) under Argon atmosphere using heating rates of 15 K/min. Mössbauer

measurements were performed at room temperature with transmission geometry using a 57Co(Rh) source of 25mCi. The velocity of Mössbauer spectra was calibrated by using a sextet of an α-Fe foil, and isomer shift (IS) values were referred to α-Fe. The spectrum was fitted with the MOSFIT program [11].

3 Results and Analysis

The phase fractions of different prepared samples as described in the previous section have been determined by XRD. Figure 1a presents the XRD pattern of the as-spun samples. The melt-spinning process directly produces the ε-phase ($\sim$100 wt.%), while Fig. 1b shows that after annealing at 500 °C for 20 min, only the τ-phase ($\sim$ 100 wt.%) is present. This result indicates that the inclusion of carbon helps to stabilize the ε-phase and allows obtaining a τ-phase subsequently after annealing in ternary $Mn_{54.3}Al_{44}C_{1.7}$ sample as reported by other researchers [12]. However, over annealing the nanocomposite at 500 and 600 °C for 20 min can led to decomposition of τ-phase and nucleation of small amount of β-Mn phase, as shown Fig. 1c, d [4]. In addition, Fig. 1c, d is found to be similar, only τ-phase ($\sim$77.7 and $\sim$75.8 wt.%) is present, except for the additional peaks related to the presence of α-Fe ($\sim$ 16.7 and $\sim$ 14.9 wt.%) and β-Mn ($\sim$ 5.6 and $\sim$ 9.3 wt.%) phases in the nanocomposite. Rietveld refinement reveals an average crystallite size of $\sim$ 60 nm for $Mn_{54.3}Al_{44}C_{1.7}$ and $\sim$ 45 nm for α-Fe phase in the as-milled powders.

Fig. 2 DSC curves of starting $Mn_{54.3}Al_{44}C_{1.7}$ (red line) and as-milled $Mn_{54.3}Al_{44}C_{1.7}/\alpha$-Fe (green line) samples, measured at a heating rate of 15 K/min
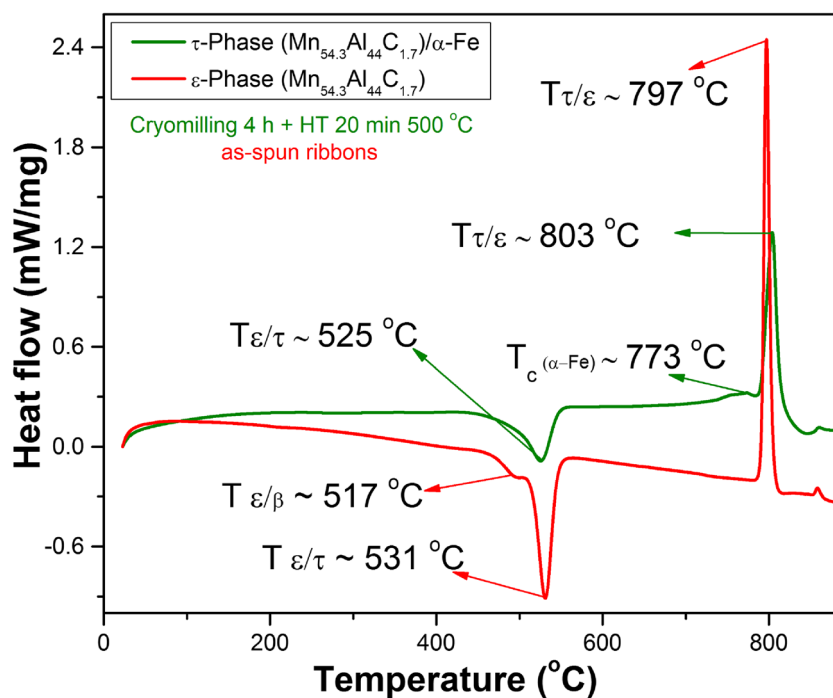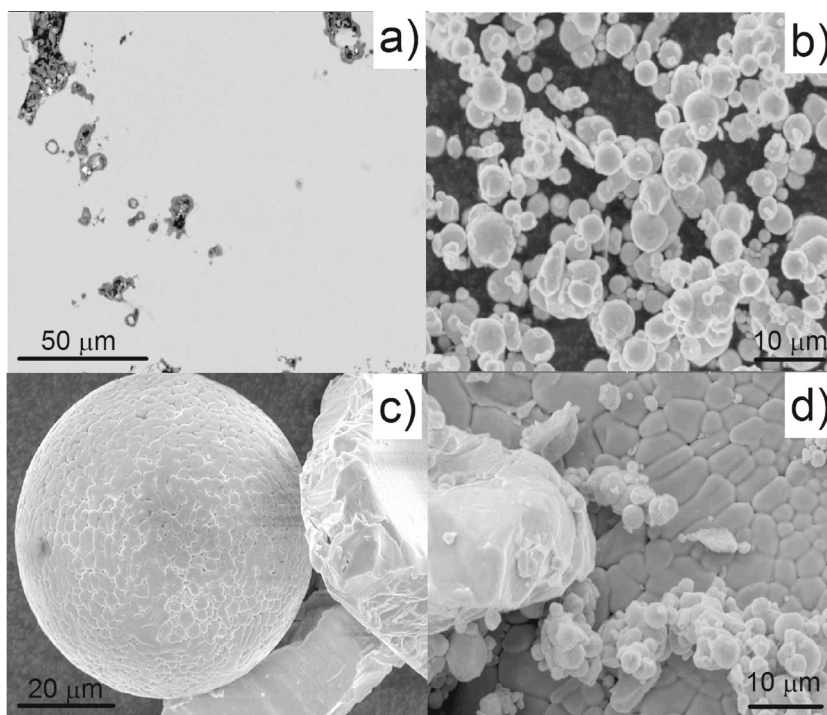
Fig. 3 SEM images of **a** $Mn_{54.3}Al_{44}C_{1.7}$ melt-spun ribbons, **b** α-Fe after cryomilling for 7 h, **c** $Mn_{54.3}Al_{44}C_{1.7}$ after cryomilling for 7 h, and **d** $Mn_{54.3}Al_{44}C_{1.7}$/α-Fe after cryomilling for 4 h and after annealing for 20 min at 500 °C

DSC curves (see Fig. 2) of $Mn_{54.3}Al_{44}C_{1.7}$ melt-spun ribbons and $Mn_{54.3}Al_{44}C_{1.7}$/α-Fe as-milled samples, reveal dominant exothermic peaks centered at 531 and 525 °C on the heating cycle, respectively, which corresponds with the annealing induced $\varepsilon \rightarrow \tau$-phase transformation, observed by Lu et al. [13]. A more complex trace is observed in the lower-temperature region (in the as-spun ribbons), where an inflection point at around $T \sim 517$ °C is detected. This behavior can be attributed to the presence of a small amount of metastable phases that are not detected by X-ray diffraction [14]. In addition, a prominent endothermic peak appears at 797 and 803 °C, which corresponds with the annealing induced $\tau \rightarrow \varepsilon$-phase transformation in the as-spun and cryomilled samples, respectively. These

Fig. 4 Hysteresis loop of starting $Mn_{54.3}Al_{44}C_{1.7}$ melt-spun ribbons (red line), $Mn_{54.3}Al_{44}C_{1.7}$ after annealing for 20 min at 500 °C (blue line), and $Mn_{54.3}Al_{44}C_{1.7}$/α-Fe after cryomilling for 4 h and after annealing for 20 min at 500 and 600 °C (green and orange line)
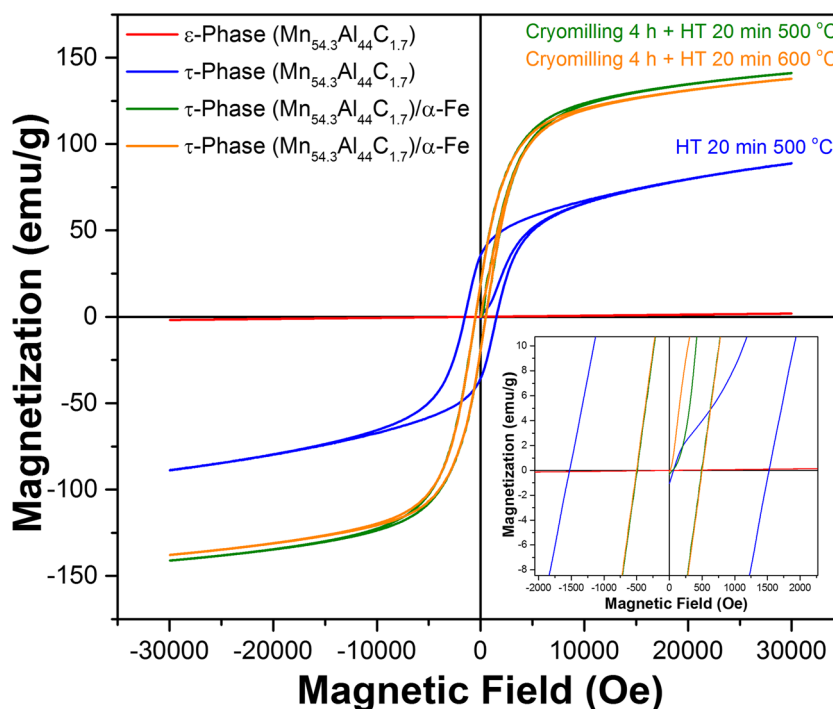
temperatures are smaller than that reported in the phase diagram of the binary Mn–Al system due the presence of C and C and Fe, respectively. These results are in good agreement with that reported by Liu et al. [14].

Figure 3a is a SEM micrograph of as-melt-spun ribbons of the $Mn_{54.3}Al_{44}C_{1.7}$ alloy. The back-scattering electron (BSE) contrast image in SEM shows no secondary phases in the as-spun state which, combined with XRD data, is an indication that pure MnAl ε-phase was obtained. Figure 3b–d presents images of the $Mn_{54.3}Al_{44}C_{1.7}$, α-Fe, and $Mn_{54.3}Al_{44}C_{1.7}/\alpha$-Fe samples after cryomilling with surfactant at different times. The higher magnification image (Fig. 3b) shows that the most significant consequence of the addition of a surfactant during the milling process is the particle size reduction and the regular morphology. According to ref. [15], for longer milling times, irregularity in the particle morphology (producing plate-like and spherical shapes) was obtained. Figure 3d shows close proximity between $Mn_{54.3}Al_{44}C_{1.7}$ and α-Fe, after cryomilling and annealing at 500 °C for 20 min.

The field-dependent magnetization measurements (Fig. 4), up to 3 T, of the $Mn_{54.3}Al_{44}C_{1.7}$ and $Mn_{54.3}Al_{44}C_{1.7}/\alpha$-Fe alloys in (i) the as-quenched state, (ii) annealed at 500 °C for 20 min, (iii) cryomilled + annealed at 500 °C for 20 min, and (iv) cryomilled + annealed at 600 °C for 20 min

are shown in Fig. 4. A magnetization value of 88 emu/g, coercivity of 1.6 kOe, and $(BH)_{max}$ of 0.66 MGOe was obtained for sample (ii), confirming the formation of pure τ-MnAl phase as indicated by the XRD data. All composite $Mn_{54.3}Al_{44}C_{1.7}/\alpha$-Fe samples (cryomilled and annealed at 500 and 600 °C for 20 min) showed ferromagnetic behavior without improvement in the coercivity values (all were $\sim$ 500 Oe), and $(BH)_{max}$ values (all were $\sim$ 0.12 MGOe) as compared with sample (ii). Nevertheless, the magnetization of these samples increased with increasing Fe content to values of 141 and 137 emu/g, for annealed samples at 500 and 600 °C, respectively.

However, from the hysteresis loops of the $Mn_{54.3}Al_{44}C_{1.7}/\alpha$-Fe samples treated at 500 and at 600 °C showed characteristic behavior of a single-phase hard magnet with no kinks in the demagnetization curve, consistent with the existence of strong intergrain exchange coupling between $Mn_{54.3}Al_{44}C_{1.7}$ and α-Fe phases. This result is similar to the reports of Saravanan et al. [16]. The Thamm-Hesse plots (Fig. 5) were obtained from the hysteresis loops at room temperature as described in [10]. Here, the Thamm-Hesse method was used to establish the type of magnetic interaction existing between magnetic particles according to the δM parameter. If $\delta M = 0$, the system is superparamagnetic or paramagnetic. For $\delta M \neq 0$, there

Fig. 5 Thamm-Hesse plots of **a** $Mn_{54.3}Al_{44}C_{1.7}$ after annealing for 20 min at 500 °C (blue line) and **b** $Mn_{54.3}Al_{44}C_{1.7}/\alpha$-Fe after cryomilling for 4 h and after annealing for 20 min at 500 and 600 °C (green and orange line)
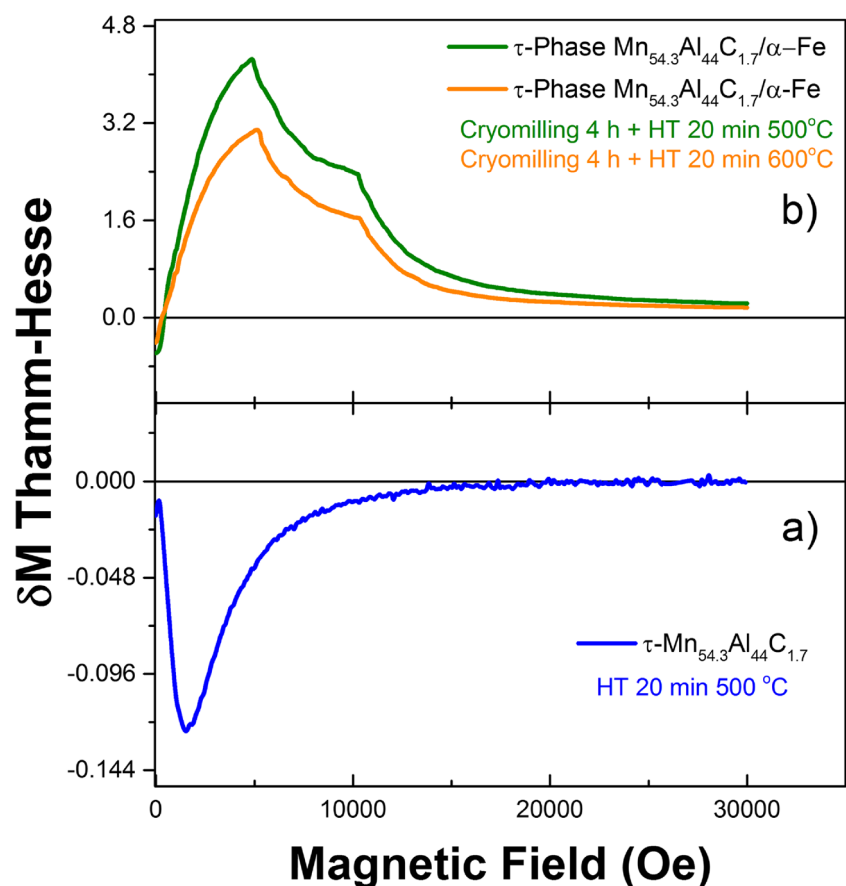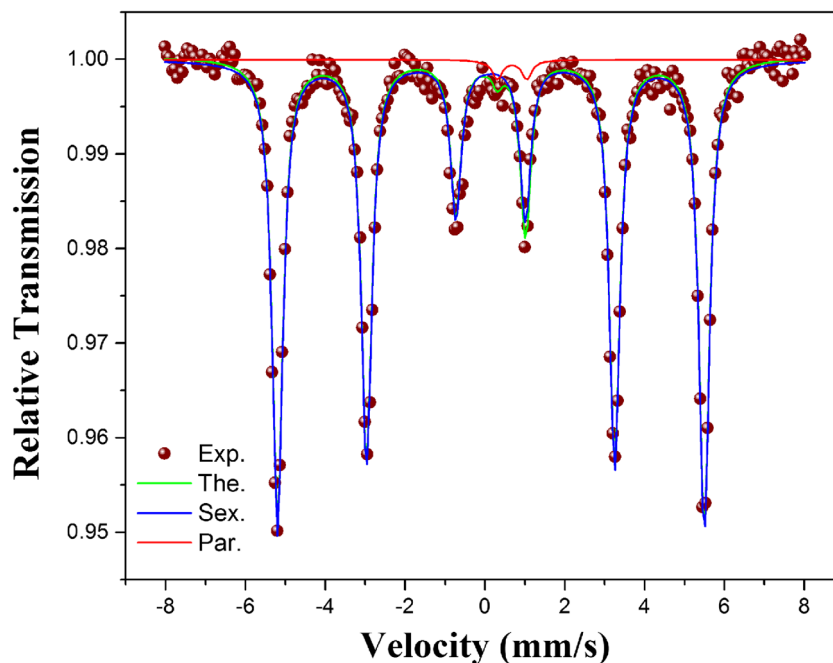
Fig. 6 Mössbauer spectra of $Mn_{54.3}Al_{44}C_{1.7}$/α-Fe after cryomilling for 4 h and after annealing for 20 min at 500 °C

are interactions between the particles or grains. In the case that $\delta M > 0$, interactions that favor magnetization prevail (exchange interaction). Finally, if $\delta M < 0$, the interactions that prevail are those that favor magnetization reversal (dipolar interaction) [17]. Then for the composite samples $Mn_{54.3}Al_{44}C_{1.7}$/α-Fe, the data show a peak splitting in the Thamm-Hesse plots. This behavior suggest that within the material, there is an intimate ferromagnetic exchange coupling between particles of the hard $Mn_{54.3}Al_{44}C_{1.7}$ phase and those of the soft α-Fe phase [17]. This effect is a consequence of the grain size refinement produced by cryomilling process. The presence of surfactant in the composite is thought to play multiple roles, including impeding cold welding of crushed particles, dispersing the powder, and preventing amorphization preserving the crystal structure [18]. In contrast, the Tamm-Hesse plot for the $Mn_{54.3}Al_{44}C_{1.7}$ sample presents negative δM values showing that the particles, which have big magnetic moment, present big magnetic dipolar interaction between them, and the majority of them are aligned antiparallel. Then the dipolar interaction prevails over the ferromagnetic exchange interaction inside the particles.

Finally, Fig. 6 shows the Mössbauer spectrum of the $Mn_{54.3}Al_{44}C_{1.7}$/α-Fe after cryomilling for 4 h and after annealing at 500 °C for 20 min. The spectrum was fitted with one sextet (mean hyperfine field ($<B_{hf}>$) = 330.5 ±0.2 kOe, isomer shift (IS) = 0.01 ±0.04 mm/s, line width (GA) = 0.32 ±0.05 mm/s, quadrupole splitting (QS) = − 0.01 ±0.05 mm/s, and area $\sim$ 98%) and one doublet (IS = 0.54 ±0.04 mm/s, GA = 0.34 ±0.05 mm/s, QS = 0.75 ±0.05 mm/s, and area $\sim$ 2%). From the fitting, it is possible

to imply that the sample exhibits a ferromagnetic behavior with broad lines caused by stresses during the milling process. The result indicates that the hyperfine parameters, obtained from the fitting procedure, match with those of α-Fe recorded at room temperature, indicating that Fe atoms are in BCC phase (as shown by XRD) and also behaves as a soft magnetic material. To improve the fit of the spectrum, it was necessary to include one doublet. According with its Mössbauer parameters, this broad doublet corresponds to a paramagnetic high-spin Fe^{3+} species [19], with Fe sites surrounded by asymmetry charge distributions (doublet); this is a consequence of the disordered character of the sample and the particle size distribution. We propose, in accordance with the XRD results, which show a Fe content of around 15% in the composite, that the origin of this paramagnetic site can correspond the small quantity of Fe that diffuse inside the hard phase.

4 Conclusions

In this work, we have studied the structural and magnetic properties of $Mn_{54.3}Al_{44}C_{1.7}$ alloys and the effect of α-Fe content on the magnetic properties of composites made from α-Fe and $Mn_{54.3}Al_{44}C_{1.7}$. A complete transformation from the ε-MnAl phase to the τ-MnAl phase was achieved after annealing at 500 °C for 20 min. The magnetization of $Mn_{54.3}Al_{44}C_{1.7}$/α-Fe composite samples increases up to $\sim$ 141 emu/g, with increased α-Fe content, but the coercivity decreases to $\sim$ 500 Oe, as compared with the coercivity of 1.6 kOe of the τ-$Mn_{54.3}Al_{44}C_{1.7}$ sample. Evidence of good

exchange coupling between $Mn_{54.3}Al_{44}C_{1.7}$ and α-Fe is observed, but future experiments are necessary to optimize processing conditions that not only will maintain the initial high coercivity but also will improve the remanence by optimizing the particle size.

References

1. Coey, J.M.: Hard magnetic materials: a perspective. IEEE Trans. Magn. **47**, 4671–4681 (2011)
2. Kuzmin, M.D., Skokov, K.P., Jian, H., Radulov, I., Gutfleisch, O.: Towards high performance permanent magnets without rare earths. J. Phys. Condens. Matter **26**, 064205 (2014)
3. Coey, J.M.: New permanent magnets; manganese compounds. J. Phys.: Condens. Matter **26**, 064211 (2014)
4. Jian, H., Skokov, K.P., Gutfleisch, O.: Microstructure and magnetic properties of Mn–Al–C alloy powders prepared by ball milling. J. Alloys Compd. **622**, 524–528 (2015)
5. Park, J., Hong, Y.K., Lee, J., Lee, W., Choi, C.J., Xu, X., Lane, A.M.: Magnetization and Intrinsic Coercivity for τ-phase Mn54Al46/α-phase Fe65Co35 composite. J. Magn. **19**(1), 55--58 (2014)
6. Wang, H.X., Si, P.Z., Jiang, W., Liu, J.J., Lee, J.G., Choi, C.J., Ge, H.L.: Structure and magnetic properties of MnAl/α-Fe nanocomposite powders prepared by high energy ball milling. Adv. Mater. Res. **287–290**, 1492–1495 (2011)
7. Kneller, E.F., Hawig, R.: The exchange-spring magnet: a new material principle for permanent magnets. IEEE Trans. Magn. **27**(4), 3588–3600 (1991)
8. Marshall, L.G., McDonald, I.J., Lewis, L.H.: Quantification of the strain-induced promotion of τ-MnAl via cryogenic milling. J. Magn. Magn. Mater. **404**, 215 (2016)
9. Larson, A.C., Von Dreele, R.B.: General structure analysis system (GSAS). Los Alamos National Laboratory Report LAUR, pp. 86–748 (2004)
10. Thamm, S., Hesse, J.: A simple plot indicating interactions between single-domain particles. J. Mag. Mag. Mat. **154**, 254–262 (1996)
11. Varret, F., Teillet, J.: Unpublished MOSFIT Program. Maine University, France (n.d.)
12. Obi, O., Burns, L., Chen, Y., Fitchorov, T., Kim, S., Hsu, K., Heiman, D., Lewis, L.H., Harris, V.G.: Magnetic and structural properties of heat-treated high-moment mechanically alloyed MnAlC powders. J. Alloys Compd. **582**, 598–602 (2014)
13. Lu, W., Niu, J., Wang, T., Xia, K., Xiang, Z., Song, Y., Mi, Z., Zhang, W., Tian, W., Yan, Y.: Phase transformations kinetics and microstructural evolutions of MnAl permanent magnet alloys. J. Alloys Compd. **685**, 992–996 (2016)
14. Liu, Z.W., Chen, C., Zheng, Z.G., Tan, B.H., Ramanujan, R.V.: Phase transitions and hard magnetic properties for rapidly solidified MnAl alloys doped with C, B, and rare earth elements. J. Mater. Sci. **47**, 2333–2338 (2012)
15. Nouri, A., Wen, C.: Surfactants in mechanical alloying/milling: a catch-22 situation. Crit. Rev. Sol. Stat. Mater. Sci. **39**, 81–108 (2014)
16. Saravanan, P., Vinod, V.T.P., Cernik, M., Chakravarty, D., Ghosal, P., Kamat, S.V.: Exchange coupled rare-earth free Mn-Al/Fe nanocomposite magnets by spark plasma sintering. Mater. Lett. **137**, 369–372 (2014)
17. Chuev, M.A., Hesse, J.: Nanomagnetism: extension of the Stoner-Wohlfarth model within Néel's ideas and useful plots. J. Phys.: Condens. Matter. **19**, 506201 (2007)
18. Cui, B.Z., Zheng, L.Y., Li, W.F., Liu, J.F., Hadjipanayis, G.C.: Single-crystal and textured polycrystalline Nd2Fe14B flakes with a submicron or nanosize thickness. Acta Mater. **60**, 1721–1730 (2012)
19. Agudelo, A.C., Marco, J.F., Gancedo, J.R., Perez Alcazar, G.A.: Fe-Mn-Al-C alloys: a study of their corrosion behaviour in SO2 environments. Hyperfine Interact. **139/140**, 141 (2002)